

From polyoxometalate building blocks to polymers and materials: the silver connection†

Yu-Fei Song,^a Hamera Abbas,^a Chris Ritchie,^a Nicola McMillian,^a De-Liang Long,^a Nikolaj Gadegaard^b and Leroy Cronin^{*a}

Received 6th December 2006, Accepted 20th February 2007

First published as an Advance Article on the web 20th March 2007

DOI: 10.1039/b617830h

Molecular growth processes utilizing polyoxometalate-based building blocks with silver connecting units have been used to produce four new materials: **1**, [Ag₃(bhepH)₈(W_{11.5}Na_{0.5}O₄₀P)₂]·8H₂O (bhep = *N,N'*-bis(2-hydroxyethyl)piperazine); **2**, [Ag₄(DMSO)₈(Mo₈O₂₆)_{*n*}]; **3**, {Ag₃[MnMo₆O₁₈{(OCH₂)₃CNH₂]₂(DMSO)₅]·3(DMSO)}_{*n*}; **4**, {Ag₃[MnMo₆O₁₈{(OCH₂)₃CNH₂]₂(DMSO)₆(CH₃CN)₂]·DMSO}_{*n*}. The compounds were characterised using single crystal X-ray crystallography, elemental analysis, IR, TGA, DSC, and compounds **2–4** were imaged on silicon substrates using scanning electron microscopy. Compound **1** represents a 0D dimer connected by silver ions but was also found to form channels facilitated by the hydrogen bonding between the protonated [bhepH]⁺ ligand and the cluster, and complex **2** forms 2D layered networks, whereas both compounds **3** and **4** form 1D networks; these networks are all connected by Ag(I) ions. Thermal studies show that the stabilities of compounds **2–4** are affected by the linking Ag(I) ions and the DMSO ligands and EM studies on compounds **3** and **4** showed the formation of fibres on silicon substrates.

Introduction

Polyoxometalate clusters (POMs) provide unrivalled structural diversity with clusters displaying a wide range of important physical properties and nuclearities, which range from 6 to 368 metal ions in a single molecule.¹ In general, POM clusters are based upon metal-oxide building blocks with a general formula of MO_{*x*} (where M is Mo, W, V and sometimes Nb, and *x* can be 4, 5, 6 or 7). POM-based materials have many interesting physical properties which result from their versatile structures, the ability to delocalise electrons over the surface of the clusters, the ability to incorporate heteroanions, electrophiles and ligands, and to encapsulate guest molecules within a metal-oxide based cage. POM clusters have been shown to exhibit catalytic activity,² ionic conductivity,³ reversible redox behaviour,⁴ and cooperative electronic phenomena.⁵ Furthermore, during the last few years, POM chemistry has become multidisciplinary,⁶ interfacing with materials science,^{7,8} nanotechnology,⁹ and biology.^{10–13}

We are interested in the 'directed' synthesis of new polyoxometalate-based clusters and in the construction of high dimensional architectures by the development of a building block approach that utilises synthetic equivalents or synthons that can be connected using pre-defined linkers.¹⁴ Whilst developing strategies towards this goal we recently reported a new family of POMs^{15–18} which appears to achieve

the first part of this goal, and allows the isolation of a new structure type by virtue of the cations used to 'encapsulate' this unit, thereby limiting its reorganisation to a simpler structure. By using this approach we have isolated {Mo₁₆}¹⁸ ≡ [H₂Mo₄Mo₁₂O₅₂]^{10–}, {M₁₈}¹⁶ ≡ [M₁₈O₅₄(SO₃)₂]^{4–} (M = Mo or W), {W₁₉}¹⁷ ≡ [H₄W₁₉O₆₄]^{6–} and {W₃₆}¹⁸ ≡ [H₁₂W₃₆O₁₂₀]^{12–} using bulky organo cations such as hexamethylenetetramine and triethanolamine. In previous work we were also able to combine the organo-cation directing approach and connect the POM-based building blocks to 1D polymeric chains, 2D grids and networks *via* coordination to electrophilic Ag(I) ions.¹⁴ As such these complexes represent rare examples of Ag-substituted POMs.^{14,19,20} By manipulating the organo counterion we could influence the overall architecture of a series of Ag–Mo POM based clusters.¹⁴ As a transition metal, silver(I) ions display a range of geometries and are able to form two to six coordination bonds, which make it a prime candidate to act as a linker.^{21,22}

In this context we describe the synthesis, structure and physical properties of four new silver-bridged polyoxometalate containing compounds (characterised by single crystal X-ray analysis, elemental analysis, infra-red spectroscopy, TGA, DSC, and SEM): **1**, [Ag₃(bhepH)₈(W_{11.5}Na_{0.5}O₄₀P)₂]·8H₂O (bhep = *N,N'*-bis(2-hydroxyethyl)piperazine); **2**, [Ag₄(DMSO)₈(Mo₈O₂₆)_{*n*}]; **3**, {Ag₃[MnMo₆O₁₈{(OCH₂)₃CNH₂]₂(DMSO)₅]·3(DMSO)}_{*n*}; **4**, {Ag₃[MnMo₆O₁₈{(OCH₂)₃CNH₂]₂(DMSO)₆(CH₃CN)₂]·DMSO}_{*n*}. Scanning electron microscopy studies on compounds **2–4** demonstrate that POM building blocks connected by silver ions can form interesting materials and thermal studies demonstrate the importance of the coordinating solvent and bridging Ag(I) linkers in dictating the overall stability of the materials. Compound **1** represents a rare example²⁰ of Ag(I) ligated to a tungsten based POM, compound

^aWestCHEM Department of Chemistry, University of Glasgow, Glasgow, UK G12 8QQ. E-mail: L. Cronin@chem.gla.ac.uk; Fax: +44 141 330 4888; Tel: +44 141 300 6650

^bDepartment of Electronics and Electrical Engineering, University of Glasgow, Glasgow, UK G12 8LT

† This paper is part of a *Journal of Materials Chemistry* issue highlighting the work of emerging investigators in materials chemistry.

2 an extension to previous work using $\{\text{Mo}_8\}$ -based building blocks but also utilises DMSO as a directing and bridging ligand in the formation of a 2D net. Compounds **3** and **4** are based upon the Anderson cluster type,²³ and have been connected to 1D chains using Ag(I) and bridging DMSO ligands but interact with the Anderson cluster *via* the tris ligand [(tris(hydroxymethyl)aminomethane)] which has three pendant hydroxyl groups that can replace the hydroxide groups on the surface of the Anderson cluster.^{23,24}

Results and discussion

Synthesis

Here we show that it is possible to generate Ag-POM-based clusters that can be constructed by utilizing synthetic equivalents and synthons as building blocks and silver(I) ions as linker groups. In compound **1**, the formation of the dimer compound is directed by using the organic cation bhep. The Keggin clusters are connected through silver(I) ions and the 0D silver-Keggin dimer units are linked further through hydrogen bonds to form an interesting silver linked tungsten based POM cluster as shown in Fig. 1. In the case of compound **2**, **3** and **4**, the building block approach has been the only way applied in the formation of the resulting 1D and 2D silver(I) coordinated POM network, though it should be noted that in compound **2**, $[\text{Mo}_6\text{O}_{19}]^{2-}$ is transformed to $[\beta\text{-Mo}_8\text{O}_{26}]^{4-}$ after complexation with AgNO_3 , and we have also observed this tendency in our related work.¹⁴

Structural studies

The structure of compound **1**, $[\text{Ag}_3(\text{bhepH})_6(\text{W}_{11.5}\text{Na}_{0.5}\text{O}_{40}\text{P})_2]$, comprises a two α -Keggin clusters bridged by a single Ag(I) *via* the terminal oxo ligands of the Keggin ion ($\text{O}-\text{Ag} = 2.571(10)$ Å and $\text{O}-\text{Ag}-\text{O}$ angle of $82.0(5)^\circ$). Although the complex is formulated as $[\text{Ag}_3(\text{bhepH})_6(\text{W}_{11.5}\text{Na}_{0.5}\text{O}_{40}\text{P})_2]$, a more accurate account is given by showing the mono-sodium substituted Keggin and full Keggin ion linked by the silver bridge, see Fig. 1: $[\text{Ag}_3(\text{bhepH})_6(\text{W}_{12}\text{O}_{40}\text{P})(\text{W}_{11}\text{Na}_1\text{O}_{40}\text{P})]$ (this

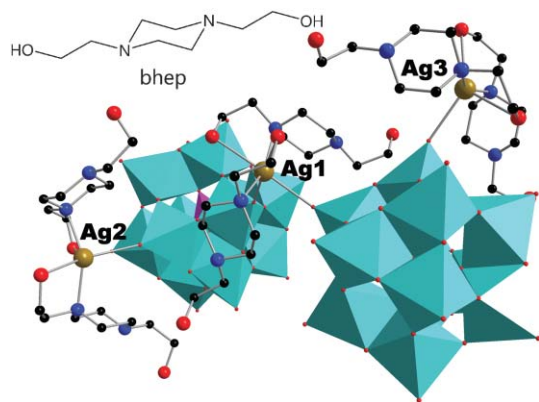


Fig. 1 Structural representation of $[\text{Ag}_3(\text{bhepH})_6(\text{W}_{11.5}\text{Na}_{0.5}\text{O}_{40}\text{P})_2]$. The W ions are shown as green polyhedra, the central P atom as a purple polyhedron. The oxo ligands in the Keggin clusters are shown as very small spheres. The bhep ligands are shown in ball and stick view (C black, N blue, O red) and the Ag(I) ion is in light brown, and the molecular structure of the bhep ligand is also shown.

is because both crystallographic and elemental analysis indicates that the tungsten positions are under-occupied and may include sodium; this was confirmed by elemental analysis). The central bridging Ag(I) ion, located on a crystallographic two-fold axis, has a distorted octahedral geometry. The $\{\text{Ag}(\text{O})_4\}$ coordination motif in the equatorial plane is defined by two oxo ligands of the Keggin ion and the two $-\text{OH}$ ligands from each of the two bhepH^+ ($\text{Ag}-\text{O} = 2.633(10)$ Å), while the axial sites of the Ag(I) ion are occupied by two nitrogen atoms from each of the bhepH^+ ligands ($\text{N}-\text{Ag} = 2.394(11)$ Å). In addition to the bridging Ag(I) ion, each Keggin is ligated to an additional non-bridging $\text{Ag}(\text{bhepH})_2$ motif where the Ag(I) ion has a distorted five coordinate geometry $\text{Ag}-\text{O}(\text{=W}) = 2.552(9)$ Å, $\text{Ag}-\text{N}$ is *ca.* 2.3 Å and the $-\text{OH}$ groups of the bhepH^+ ligand are ligated at longer distances that average *ca.* 2.724 Å. The cluster dimer units are also involved in an extensive hydrogen-bonded network which forms a channel-like structure containing a large amount of solvent water molecules, see Fig. 2.

Compound **2** can be formulated as $[\text{Ag}_4(\text{DMSO})_8(\text{Mo}_8\text{O}_{26})_n]$ and related to the chain-like structures published previously containing polymers based on the $\{\text{Ag}-\text{Mo}_8-\text{Ag}\}$ synthon.¹⁴ However, in this case, these synthons do not link together to form a chain-like arrangement but instead DMSO solvent is incorporated into the structure and also ‘pillars’ the $\text{Ag}-\text{Mo}$ POM fragments, which ligate a total of four Ag(I) ions per cluster, providing essential support to the overall network. The $\{\text{Mo}_8-\text{Ag}_4\}$ building block is arranged in such a way that it extends into a two-dimensional network *via* the coordinated DMSO molecules, see Fig. 3.

The $\{\text{Mo}_8\}$ unit is ligated by Ag(I) ions on four of the six faces of the cluster and the clusters are connected *via* bridging DMSO solvents which are ligated to the Ag(I) ions present in the $\{\text{Mo}_8\text{Ag}_4\}$ units and are coordinated alternately by S and O donor atoms.

Further, Ag(I) is bound to four oxygen atoms of the $[\text{Mo}_8\text{O}_{26}]^{4-}$ fragment and to two oxygens of two DMSO

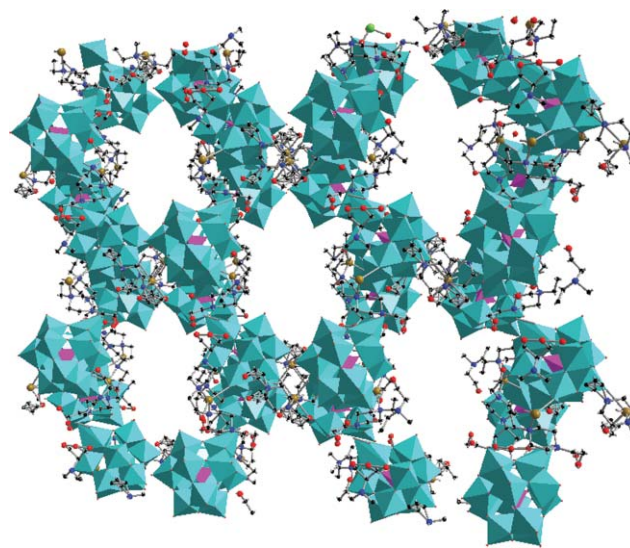


Fig. 2 Structural representation of the packing diagram for $[\text{Ag}_3(\text{bhepH})_6(\text{W}_{11.5}\text{Na}_{0.5}\text{O}_{40}\text{P})_2]$. Colour scheme as in Fig. 2. The solvent water molecules are omitted and the cavities that run through the structure are clearly seen.

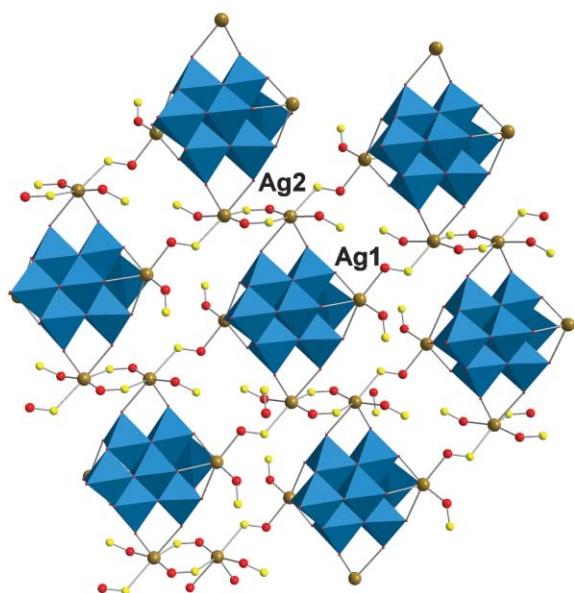


Fig. 3 Structural representation of $[Ag_4(DMSO)_8(Mo_8O_{26})]_n$. The Mo positions are shown as blue polyhedra, the Ag(I) ions in brown, S = yellow, O = red, carbon atoms and solvents omitted. Average Ag–O(Mo) bond distances between the ‘ends’ of the cluster (Ag1) fall within the range 2.298–2.751 Å whereas in the ‘middle’ (Ag2) the distances are in the range 2.346–2.873 Å.

molecules resulting in the Ag centre in an octahedral environment with a trigonally distorted geometry. The O–Ag–O angles and Ag–O bond distances fall within the expected ranges of 74.15(7) to 151.89(9)° and 2.296(3) to 2.581(2) Å respectively. In addition to this, one of the DMSO molecules is further coordinated to another silver (Ag(2)) ion through a Ag–S bond bringing the total number of silver ions in the asymmetric unit to two. The silver in this ‘linker’ unit links the Ag–Mo POM unit together in a two-dimensional array. The Ag(2) ion is also in an octahedral environment with trigonal distortion and on closer inspection is actually linked to a total number of four DMSO molecules either through Ag–O bonds or Ag–S bonds. The O–Ag–S angles are 76.96(6) to 119.56(6)° with Ag–O bond distances of 2.343(2) to 2.449(2) Å, see Fig. 3. In summary this 2D network comprises $\{Mo_8Ag_4\}$ units that are connected by 4 DMSO ligands and also contain 4 non-bridging DMSO ligands.

Compound **3**, $\{Ag_3[MnMo_6O_{18}\{(OCH_2)_3CNH_2\}_2(DMSO)_5] \cdot 3(DMSO)\}_n$, forms a 1D chain in the solid state where the repeat unit in the chain is built from two tris-derived Anderson cluster $[MnMo_6O_{18}\{(OCH_2)_3CNH_2\}_2]^{3-}$ units connected *via* a bridging $\{Ag_2(DMSO)_4\}^{2+}$ unit and the chain is propagated by a single Ag(I) which connects the nitrogen atom of the tris ligands. A further $\{Ag(DMSO)_3\}^+$ unit decorates the Anderson cluster, see Fig. 4.

The Ag–N in the N–Ag–N moiety is bound at a distance of 2.175(6) Å and the N–Ag–N angle is 173.4(2)°. The Ag(I) ions present in the $\{Ag_2(DMSO)_4\}^{2+}$ unit have a five coordinate geometry and the Ag–O(Mo) distances are in the range 2.425–2.488 Å. The DMSO ligands bridge each of the Ag(I) ions *via* an Ag–O interaction and these distances range from 2.298 to 2.479 Å and the Ag–O–Ag angle is 95.97°. The final decorating

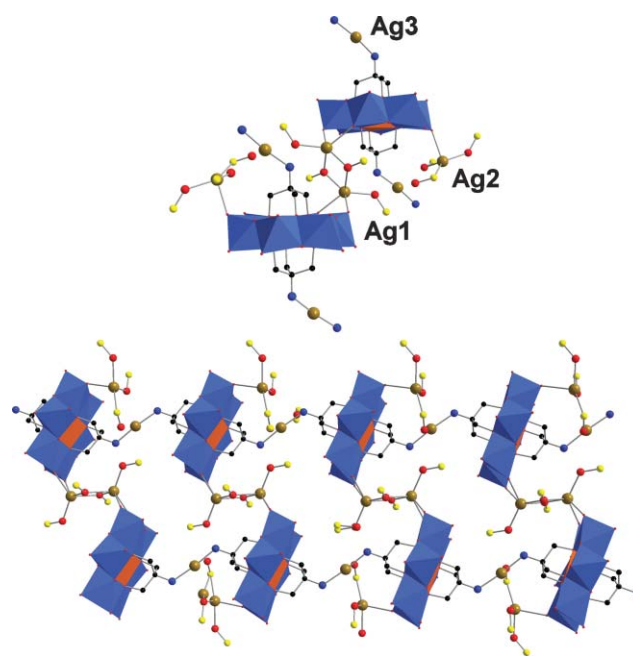


Fig. 4 Structural representations of $Ag_3[MnMo_6O_{18}\{(OCH_2)_3CNH_2\}_2(DMSO)_5]$. Top: A repeat unit of the polymeric framework is shown. The two clusters are bridged by a $\{Ag_2(DMSO)_4\}^{2+}$ unit and the chain grows *via* linear Ag(I) that bridges the two nitrogen atoms of the tris ligand that is capping the cluster. Bottom: The 1D chain formed by the N–Ag–N interactions is shown. The Mo and Mn positions are shown as blue and orange polyhedra respectively, the Ag(I) ions in brown, S = yellow, O = red, C = black, N = blue; solvent, and carbon atoms of the DMSO ligands omitted.

$\{Ag(DMSO)_3\}^+$ comprises a 4 coordinate Ag(I) with a Ag–O(Mo) distance of 2.552 Å. This 1D network therefore incorporates 2 bridging and 3 terminally coordinated DMSO ligands.

Compound **4**, like compound **3**, also comprises the tris-Anderson building block and can be formulated as $\{Ag_3[MnMo_6O_{18}\{(OCH_2)_3CNH_2\}_2(DMSO)_6(CH_3CN)_2] \cdot DMSO\}_n$. This compound is also a 1D chain in the solid state where the repeating unit in the chain is built from one type of tris-derived Anderson cluster $[MnMo_6O_{18}\{(OCH_2)_3CNH_2\}_2]^{3-}$ units combined with Ag(I) and DMSO ligands. However in this case, the tris ligand on each side of the cluster (see Fig. 4) acts differently. The tris ligands on the right side of the cluster are defined as ‘tail’ groups and here are non-bridging instead of ligating $\{Ag(CH_3CN)_2(DMSO)\}^+$; the Ag(3) ion is in a 4 coordinate coordination mode and the Ag–N distance is 2.239 Å, see Fig. 5. The *tris* group on the left side of the cluster acts as a ‘head’ group and ligates to Ag(2) and the Ag–N distance is 2.258 Å. This Ag ion is itself part of a $\{Ag_2(DMSO)_4\}^{2+}$, see Fig. 5. Two DMSO ligands (*via* the oxo groups) bridge between Ag2 and Ag1 which itself is ligated to the side of the adjacent cluster in the 1D polymer with Ag–O(Mo) distances that fall in the range 2.414–2.680 Å.

Thermal studies

To investigate the stability of these silver-polyoxometalate-based materials a series of TGA and DSC experiments were

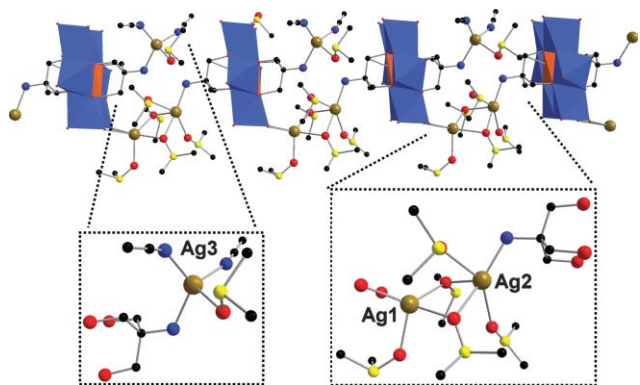


Fig. 5 Structural representation of compound **4** $\{Ag_3[MnMo_6O_{18}\{(OCH_2)_3CNH_2\}_2(DMSO)_6(CH_3CN)_2] \cdot DMSO\}_n$. This is also a 1D coordination polymer but the Anderson-tris cluster units are linked together in a head to tail fashion. The tris ligand on the right side of the cluster is terminated with a $\{Ag(CH_3CN)_2(DMSO)\}^+$ unit (see bottom left insert) whereas the tris ligand on the left side of the cluster connects to the adjacent cluster *via* a $\{Ag_2(DMSO)_4\}^{2+}$ linker unit (see bottom right insert). The Mo positions and Mn are shown as blue and orange polyhedra respectively, the Ag(I) ions in brown, S = yellow, O = red, C = black, N = blue; solvent omitted.

undertaken to see what effect the different building blocks would have on the stability of the materials produced. Both TGA and DSC studies were undertaken on compounds **1–4** and these results are summarised in Fig. 6.

The studies on compound **1** confirm the porous nature of the material with the initial weight loss of 13% corresponding to the loss of water from the solvent accessible cavity present. Both the TGA and DSC traces show the decomposition of the bhepH ligand in a series of steps. Compound **2** shows two well defined regions of solvent loss each corresponding to the loss of 4 DMSO molecules per event. The initial solvent loss appears to be the terminal DMSO ligands present and is well correlated with a sharp ‘melting’ like event in the DSC at *ca.* 150 °C. Compound **3** also shows a well defined series of events in the TGA associated with DMSO loss where the first two events correspond to the terminal and solvent DMSO being lost (5 DMSO) and the third event appears to be associated with the loss of the bridging ligands (3 DMSO). Again the DSC shows a ‘melting’ like event at *ca.* 150 °C associated with the first set of solvent loss. Compound **4** is also similar with loss of solvent DMSO, CH_3CN and terminal DMSO. The bridging DMSO ligands are lost next. Once again the DSC shows a ‘melting’ like event at *ca.* 150 °C.

It is interesting that all the silver-based coordination polymers demonstrated a degree of similar stability and behaviour despite the different types of polymer and bridging modes present. In particular the appearance of the sharp DSC ‘melting’ like event at *ca.* 150 °C for compounds **2–4** is intriguing. It would appear that the DMSO ligands present in **2–4** probably account for the similar results associated with the loss of solvent, terminal and bridging ligands with the solvent/terminal ligands being lost below 150 °C and the bridging DMSO ligands being lost at temperatures high than 200 °C.

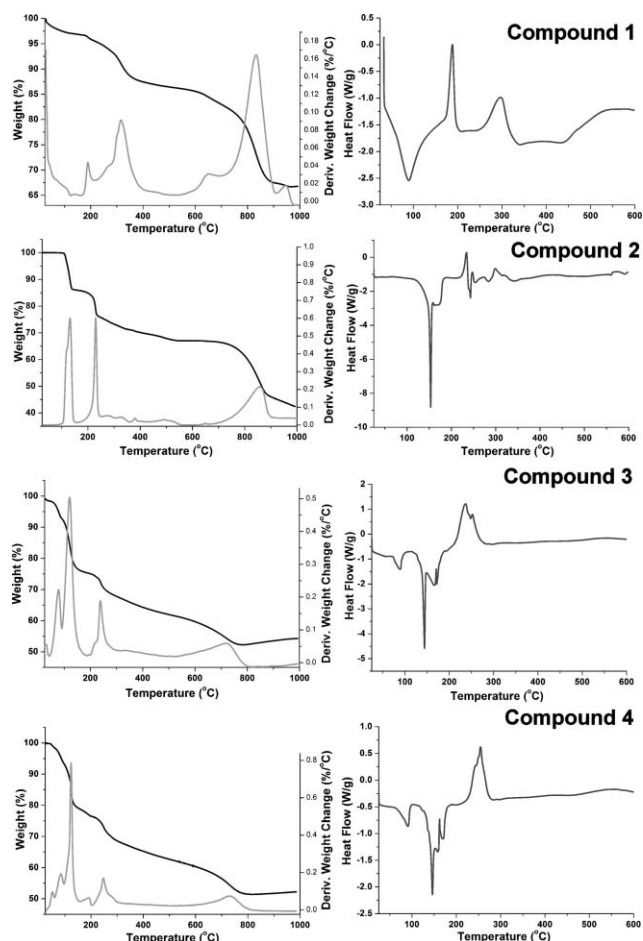


Fig. 6 TGA traces on the left side (weight loss in black and derivative in grey) and DSC traces on the right side for compounds: **1**, $[Ag_3(bhepH)_8(W_{11.5}Na_{0.5}O_{40}P)_2] \cdot 8H_2O$; **2**, $[Ag_4(DMSO)_8(Mo_8O_{26})]_n$; **3**, $\{Ag_3[MnMo_6O_{18}\{(OCH_2)_3CNH_2\}_2(DMSO)_5] \cdot 3(DMSO)\}_n$; **4**, $\{Ag_3[MnMo_6O_{18}\{(OCH_2)_3CNH_2\}_2(DMSO)_6(CH_3CN)_2] \cdot DMSO\}_n$.

Scanning electron microscopy studies

Compound **2** has been shown to deposit on silicon in a crystalline fashion and the layered nature of the material can clearly be seen, see Fig. 7.

In contrast deposition of compounds **3** and **4** produced very similar results, giving fibres which are less than 0.5 μm thick and over 10 μm long on average (Fig. 8). These fibres were simply produced by dissolving compounds **3** and **4** in CH_3CN and evaporating a drop onto a freshly cleaned silicon

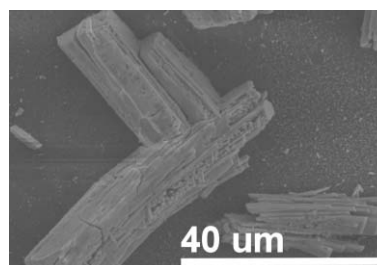


Fig. 7 SEM of compound **2**. The layered nature of the material can be seen and delamination of the crystallites can also be observed.

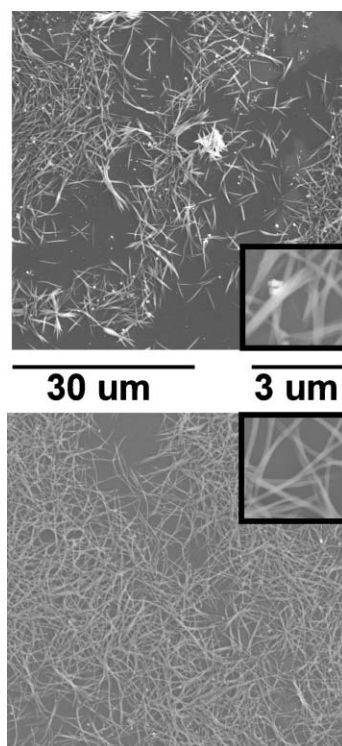


Fig. 8 SEM images of compounds **3** (top) and **4** (bottom). Both compounds appear to give fibres which are at least 10 μm long although compound **4** appears to give longer and thinner fibres on average.

substrate. EDX analysis of both sets of substrates from experiments with compounds **3** and **4** confirmed the presence of Mo, Ag, and O in the proportions expected for compounds **3** and **4** respectively (data not shown).

Conclusions

This work demonstrates a strategy to control the molecular growth processes by connecting anionic polyoxometalate building blocks using silver(I)-based linkers, and therefore has extended the rare class of silver containing polyoxometalate materials.^{14,19,20} By using a building block approach a range of materials (**1–4**) have been produced which vary in dimensionality from 0D to 1D and 2D networks. Furthermore the stability of these materials was found to be crucially dependent on the presence of the silver and DMSO coordinating ligand rather than the types of polyoxometalate building block present. Surface studies of the deposition of compounds **3–4** on silicon substrates yielded some interesting observations which indicate that the 1D coordination polymers seen crystallographically also form fibres on the surface $>10 \mu\text{m}$ in length with a diameter of *ca.* 0.5 μm . This means that the derivatised Anderson cluster appears to be a robust and useful building block with potential for use in the self assembly of functional materials, which is of great interest in many areas of chemistry. Given the versatile electronic properties of POMs, this building block approach might become relevant, *e.g.* the production of spacers of specific dimensionality for use as a skeleton for conducting interconnectors in nanoscale electronic devices, or as e^- -beam resists. Future work will therefore

concentrate on extending this molecular growth strategy to other POM-based structures linking the crystallographically determined building block principles to real materials.

Experimental

Synthesis

Compound 1. $[\text{Ag}_3(\text{bhepH})_8(\text{W}_{11.5}\text{Na}_{0.5}\text{O}_{40}\text{P})_2] \cdot 8\text{H}_2\text{O} \cdot \text{Na}_2\text{WO}_4 \cdot 2\text{H}_2\text{O}$ (1.65 g, 5.0 mmol) was dissolved in water (20 mL) and acidified to pH 4 with 4 M HNO_3 . To this solution was added *N,N'*-bis(2-hydroxyethyl)piperazine (0.84 g, 4.82 mmol) and the pH was increased to 7. Upon the addition of H_3PO_4 (0.44 g) the pH decreased to 6.47. Finally a solution of AgNO_3 (165 mg, 0.97 mmol) in water (1 mL) was added dropwise which resulted in the formation of a yellow precipitate. The solution was centrifuged several times and the clear solution decanted into a separate flask. The solution continued to precipitate but on leaving for several days produced clusters of white needles in spherulite formation, which were suitable for single crystal X-ray diffraction. Yield: 300 mg (19% yield based on W). $\text{C}_{64}\text{H}_{168}\text{Ag}_3\text{N}_{16}\text{O}_{104}\text{P}_2\text{W}_{23}\text{Na}$: found (calc.) %: C 9.95 (10.30), H 2.14 (2.27), N 2.86 (3.00); IR (KBr, cm^{-1}): 3425 (b), 3009 (w), 2960 (w), 2847 (w), 2721 (w), 1626 (w), 1457 (s), 1276 (s), 1190 (w), 1122 (w), 1078 (vs), 1034 (vs), 945 (vs), 851 (vs), 802 (vs), 727 (vs).

Compound 2. $[\text{Ag}_4(\text{DMSO})_8(\text{Mo}_8\text{O}_{26})_n]$: Silver(I) nitrate (23 mg, 0.14 mmol) in DMSO (2 mL) was added dropwise to a solution of $((n\text{-C}_5\text{H}_{11})_4\text{N})_2\text{Mo}_6\text{O}_{19}$ (102 mg, 0.069 mmol) in DMSO (5 mL) and then acetone was added (0.01 mL). The mixture was covered, and left for 48 hours to stir at room temperature. After this time the solution was still transparent yellow. Large colourless block crystals were successfully grown by diffusion of ethanol over 10 days. The crystals were suitable for single crystal X-ray diffraction. Yield: 48 mg (31%). $\text{C}_{16}\text{H}_{48}\text{Ag}_4\text{Mo}_8\text{O}_{34}\text{S}_8$: found (calc.) %: C 8.59 (8.59), H 2.17 (2.16); IR (KBr, cm^{-1}): 3432 (b), 2996 (m), 1634 (m), 1435 (m), 1402 (m), 1311 (m), 1026 (s), 944 (s), 914 (s), 841 (s), 711 (s).

Compound 3. $\{\text{Ag}_3[\text{MnMo}_6\text{O}_{18}\{(\text{OCH}_2)_3\text{CNH}_2\}_2(\text{DMSO})_5] \cdot 3(\text{DMSO})\}_n$: AgNO_3 (0.18 g, 1.06 mmol) in 10 mL of MeOH was added to Mn-Anderson cluster (0.5 g, 0.26 mmol) in 10 mL of DMSO. Yellow precipitates were formed immediately. The solution was kept stirring at 60 $^\circ\text{C}$ for 10 mins and another 10 mL of DMSO was added in. The solution was kept in dark for slow evaporation and yellow crystals were obtained after 3 days. Yield: 80 mg (15%). Elemental analysis: found (calc.) %: C 13.52 (13.70), H 3.45 (3.07) N 1.57 (1.33). $\text{C}_{24}\text{H}_{64}\text{O}_{32}\text{N}_2\text{S}_8\text{Ag}_3\text{MnMo}_6$ (2103.47). IR (KBr, cm^{-1}): 1680 (w), 1595 (w), 1445 (w), 1315(w), 1040 (s), 1000 (s), 937 (s), 903 (s), 693 (m), 565 (m)

Compound 4. $\{\text{Ag}_3[\text{MnMo}_6\text{O}_{18}\{(\text{OCH}_2)_3\text{CNH}_2\}_2(\text{DMSO})_6(\text{CH}_3\text{CN})_2] \cdot \text{DMSO}\}_n$: Mn-Anderson cluster (0.50 g, 0.26 mmol) was dissolved in 10 mL of MeCN, to which AgCF_3SO_3 (0.27 g, 1.06 mmol) in 10 mL of DMSO was added. Yellow precipitates were generated immediately. The solution was warmed to 50 $^\circ\text{C}$ and another 10 mL of DMSO was

Table 1 Crystallographic data for compounds 1–4

	1	2	3	4
Formula	C ₆₄ H ₁₆₈ Ag ₃ W ₂₃ Na ₁ N ₁₆ O ₁₀₄ P ₂	C ₁₆ H ₄₈ Ag ₄ Mo ₈ O ₃₄ S ₈	C ₂₄ H ₆₄ Ag ₃ Mo ₆ N ₂ O ₃₂ S ₈	C ₂₆ H ₆₄ Ag ₃ Mo ₆ N ₄ O ₃₁ S ₇
<i>M_r</i> /g mol ⁻¹	7463.23	2240.02	2103.44	2107.42
Crystal system	Monoclinic	Triclinic	Monoclinic	Monoclinic
Space group	<i>C2/c</i>	<i>P</i> $\bar{1}$	<i>P2₁/n</i>	<i>P2₁/n</i>
<i>a</i> /Å	32.777(2)	10.8053(3)	11.9401(3)	11.984(4)
<i>b</i> /Å	24.7371(15)	11.1381(3)	38.3746(10)	37.696(10)
<i>c</i> /Å	23.2352(14)	13.3396(3)	12.8124(3)	13.122(4)
α /°	90	97.200(2)	90	90
β /°	111.181(3)	113.4870(10)	94.095(2)	97.158(15)
γ /°	90	108.7740(10)	90	90
<i>V</i> /Å ³	17566.5(19)	1333.30(6)	5855.6(3)	5882(3)
<i>Z</i>	4	1	4	4
ρ_{calc} /g cm ⁻³	2.864	2.790	2.386	2.380
$\mu(\text{MoK}\alpha)$ /mm ⁻¹	15.43	3.646	2.797	2.751
<i>T</i> /K	100(2)	150(2)	120(2)	100(2)
No. rflns (measd)	68734	18453	26806	43546
No. rflns (indep)	15393	5233	10369	9324
No. rflns (obsd)	8997	4664	7582	5577
No. params	850	317	726	665
<i>R</i> 1 (<i>I</i> > 2 σ (<i>I</i>))	0.0594	0.0249	0.0444	0.0664
<i>wR</i> 2 (all data)	0.1861	0.0600	0.0948	0.1531

added. A small amount of precipitate was filtered off and the solution was left in the dark for slow evaporation. Yellow crystals were obtained after one week. Yield: 98 mg (18%). Elemental analysis: found (calc.) %: C 15.20 (14.82), H 3.26 (3.06), N 2.88 (2.66). C₂₆H₆₄O₃₁N₄S₇Ag₃MnMo₆ (2107.44). IR (KBr, cm⁻¹): 3425 (br), 1655 (w), 1439 (m), 1312 (w), 1031 (s), 938 (s), 907 (s), 671 (s), 642 (s), 562 (w).

X-Ray crystallographic studies

Data were measured on a Bruker Apex CCD diffractometer [$\lambda(\text{MoK}\alpha) = 0.71073 \text{ \AA}$], graphite monochromator. Structure solution was with SHELXS-97 and refinement with SHELXL-97. See Table 1 for summary crystallographic data.

CCDC reference numbers 629954–629957. For crystallographic data in CIF or other electronic format see DOI: 10.1039/b617830h

Scanning electron microscope (SEM) measurements

The silicon substrates were cleaned and prepared by sonication in ethanol for 20 minutes. Then solutions of 2–4 were made up to 1 mg mL⁻¹ in CH₃CN and then 10 μ L of the solution was deposited onto the substrate and dried. The SEM images were obtained by using a field emission SEM (JEOL, JSM-6400) operated at an acceleration voltage of 10 kV.

Thermal analysis data

TGA data were collected on a TA instruments Q 500 thermal analyser under nitrogen carrier gas. The ramp rate was 2 °C min⁻¹ to 200 °C and then 10 °C min⁻¹ to 1000 °C. The DSC measurements were done on a TA instruments DSC Q 600. The ramp rate was 5 °C min⁻¹ and the sample was placed in an aluminium pan.

Acknowledgements

We would like to thank the EPSRC, Royal Society, The University of Glasgow and WestCHEM for funding.

References

- 1 A. Müller, E. Krickemeyer, J. Meyer, H. Bogge, F. Peters, W. Plass, E. Diemann, S. Dillinger, F. Nonnenbruch, M. Randerath and C. Menke, *Angew. Chem., Int. Ed. Engl.*, 1995, **34**, 2122.
- 2 R. Neumann and M. Dahan, *Nature*, 1997, **388**, 353; N. Mizuno and M. Misono, *Chem. Rev.*, 1998, **98**, 199.
- 3 D. E. Katsoulis, *Chem. Rev.*, 1998, **98**, 359; T. Yamase, *Chem. Rev.*, 1998, **98**, 307.
- 4 T. Rütger, V. M. Hultgren, B. P. Timko, A. M. Bond, W. R. Jackson and A. G. Wedd, *J. Am. Chem. Soc.*, 2003, **125**, 10133.
- 5 E. Coronado, C. Gimenez-Saiz, C. J. Gomez-Garcia and S. C. Capelli, *Angew. Chem., Int. Ed.*, 2004, **43**, 3022.
- 6 M. T. Pope and A. Müller, *Angew. Chem., Int. Ed. Engl.*, 1991, **30**, 34.
- 7 N. Casan-Pastor and P. Gomez-Romero, *Front. Biosci.*, 2004, **9**, 1759.
- 8 M. I. Khan, *J. Solid State Chem.*, 2000, **152**, 105.
- 9 D.-L. Long and L. Cronin, *Chem.-Eur. J.*, 2006, **12**, 3698.
- 10 H. Y. Ma, J. Peng, Z. G. Han, X. Yu and B. X. Dong, *J. Solid State Chem.*, 2005, **178**, 3735.
- 11 T. Yamase, *J. Mater. Chem.*, 2005, **15**, 4773.
- 12 B. Hasenknopf, *Front. Biosci.*, 2005, **10**, 275.
- 13 K. Nomiya, H. Torii, T. Hasegawa, Y. Nemoto, K. Nomura, K. Hashino, M. Uchida, Y. Kato, K. Shimizu and M. Oda, *J. Inorg. Biochem.*, 2001, **86**, 657.
- 14 H. Abbas, A. L. Pickering, D.-L. Long, P. Kogerler and L. Cronin, *Chem.-Eur. J.*, 2005, **11**, 1071.
- 15 (a) D.-L. Long, P. Kogerler, L. J. Farrugia and L. Cronin, *Dalton Trans.*, 2005, 1372; (b) D. L. Long, P. Kogerler, L. J. Farrugia and L. Cronin, *Angew. Chem., Int. Ed.*, 2003, **42**, 4180.
- 16 D.-L. Long, P. Kogerler and L. Cronin, *Angew. Chem., Int. Ed.*, 2004, **43**, 1817.
- 17 D.-L. Long, P. Kogerler, A. D. C. Parenty, J. Fielden and L. Cronin, *Angew. Chem., Int. Ed.*, 2006, **45**, 4798–4803.
- 18 D.-L. Long, O. Brücher, C. Streb and L. Cronin, *Dalton Trans.*, 2006, 2852; D. L. Long, H. Abbas, P. Kogerler and L. Cronin, *J. Am. Chem. Soc.*, 2004, **126**, 13880.
- 19 S.-M. Chen, C. Z. Lu, Y.-Q. Yu, Q.-Z. Zhang and X. He, *Inorg. Chem. Commun.*, 2004, **7**, 1041.
- 20 H. I. S. Nogueira, F. A. A. Paz, P. A. F. Teixeira and J. Klinowski, *Chem. Commun.*, 2006, 2953.
- 21 A. L. Pickering, D.-L. Long and L. Cronin, *Inorg. Chem.*, 2004, **43**(16), 4953.
- 22 R. Villanneau, A. Proust and F. Robert, *Chem. Commun.*, 1998, 1491.
- 23 S. Favette, B. Hasenknopf, J. Vaissermann, P. Gouzerh and C. Roux, *Chem. Commun.*, 2003, 2664.
- 24 B. Hasenknopf, R. Delmont, P. Herson and P. Gouzerh, *Eur. J. Inorg. Chem.*, 2002, 1081.